[Article ID] 1003- 6326(2002)05- 0931- 05

Effect of preferential dissolution on erosion-corrosion for chromium steel in alkali slurry①

YUAN Qing-long (袁庆龙)[1], M. M. Stack[2]
(1. Surface Engineering Research Institute,
Taiyuan University of Technology, Taiyuan 030024, China;
2. Department of Mechanical Engineering, University of Strathclyde, Glasgow G11XJ, UK)

[Abstract] An investigation was carried out concerning the effect of preferential dissolution on the erosion-corrosion for a chromium steel in 1 mol/L NaOH. Preliminary tests using a potentiodynamic technique were performed in order to establish the presence of preferential dissolution in the alkali solution with and without the alumina particles at different rotation speeds. For purposes of quantifying the observed phenomena a potentiostatic mass loss method was also used. The results show that the active peaks occur at potential between + 0.4 and + 0.5 V on the polarization curves, which indicates that there is a preferential dissolution for chromium steel under erosion-corrosion conditions and the ferrite phase acts as a sacrificial anode in favor of $(Fe, Cr)_7C_3$ phase. Addition of particles can promote the preferential dissolution at different rotation speeds. The combined effects of erosion-corrosion results in total mass loss rates to be greater than the sum effects of each process taken alone, thus showing a strong synergism between erosion and corrosion due to preferential dissolution.

[Key words] chromium steel; erosion-corrosion; preferential dissolution; synergism
[CLC number] TG 172.85 [Document code] A

1 INTRODUCTION

In the Bayer process, in hydroelectric power plants and in offshore piping systems, flowing corrosion media often contain solid particles. These solid particles suspended in liquid form slurries, and the process of slurry erosion-corrosion can be particularly destructive. Under these environments, the surfaces of components are damaged not only by the scouring action of the solid particles, but also by the electrochemical corrosion. Both erosion and corrosion processes may act synergistically to produce an overall effect that is greater or less than the sum of the damage caused by each process acting independently. There was a great deal of interest in this phenomenon[1~5]. Mutsumura[5,6] determined that synergy existed during the erosion-corrosion of stainless steel and iron in both acids and alkali, with corrosion accelerating the erosion. This was attributed to dissolution of the work hardened layer and an increase in surface roughness causing more destructive erosion impacts. Corrosion was also reported to be inhibited by erosion due to the production of impact craters having crystal planes on which dissolution was slower. It was considered, however, that the conclusions made may not be accurate due to an inability to resolve the various variables of erosion and corrosion, a problem that was acknowledged[6]. Li et al[3] also found a synergism to be present in the erosion-corrosion of aluminum over a range of pH value, with the main effect arising from corrosion enhanced erosion. The specific mechanism of enhancement was concluded to be enhanced crack growth rate in the surface oxide though precise determination was not possible.

Yue et al[7] detailed a mechanism for describing the interaction between erosion and corrosion in aqueous condition:

$$K_{e\text{-}c} = K_c + K_e + \Delta K_c + \Delta K_e \quad (1)$$

where $K_{e\text{-}c}$ is the erosion-corrosion rate, K_c is the pure corrosion rate, K_e is the pure erosion rate, ΔK_c is corrosion rate increment, and ΔK_e is erosion rate increment. If $K_{e\text{-}c} = K_c + K_e + \Delta K_c$, then the erosion-corrosion is considered to be "additive" (erosion enhanced corrosion). If this is not the case, then a synergistic effect is observed, that is of corrosion enhancing the erosion. However, few have determined the separate contributions of erosion and corrosion to the overall rate.

For the stainless steels, preferential dissolution is well known, which occurs when different components of an alloy, or when different phases of a multiphase material, corrode at different rates. However, the effect of preferential dissolution on erosion was not always taken into consideration. In present work, the polarization curves are determined and used in order to define the behavior of a chromium steel within a certain range of potentials (active corrosion) in alkali slurries of different particle sizes with respect to preferential dissolution and the reason for preferential dissolution to accelerate the erosion is discussed.

2 EXPERIMENTAL

2.1 Apparatus

A rotation cylinder electrode (RCE) apparatus was used for the erosion-corrosion tests, which is schematically shown in Fig. 1. The RCE rig consists

① [Received date] 2002- 03- 05; [Accepted date] 2002- 05- 16

of a hollow cylindrical working electrode (specimen ring), an auxiliary counter electrode (platinum foil), both contained in the electrode cell, and an outside standard reference electrode (Hg/HgO) connected to the solution by a salt bridge. Electrical connection to the cell, made through the three electrodes, is controlled by an ACM potentiostat. Signal inputs to and data acquisition from the potentiostat were carried out by a control computer via a high velocity digital-to-analogue (D/A) and analogue-to-digital (A/D) conversion interface board interfaced by an Easyest LX software.

2.2 Material and experimental conditions

The material tested was a chromium steel which has a chemical composition of 0.13%~0.18%C, 0.51%Mn, 0.44%Si, 0.46%Al, 12.0%Cr and balance Fe. The specimens were machined to a final dimension of 38 mm (outer diameter) × 2~4 mm (wall thickness) × 10 mm (height). Prior to testing, the specimen surface was finished with silicon carbide abrasive paper, rinsed in de-ionized water, degreased in acetone, dried in air and weighted. After testing, the specimen was cleaned, removed and re-weighted.

The slurries, based on the 1 mol/L NaOH solutions, were prepared from de-ionized water and sufficient deaerated using pressurized nitrogen, contained 50 μm, 100 μm and 150 μm alumina particles with nominal concentration of 275 g/L respectively. In-situ purging of nitrogen into the cell was further made during the wear test through an upper inlet to the cell which can avoid possible cavitation erosion associated with nitrogen bubbling via a lower inlet. The test was carried out at ambient temperatures and a water bath was used for the high-speed rotation test to prevent significant slurry temperature rises.

2.3 Potentiodynamic sweeps

Polarization curves in 1 mol/L NaOH solution with and without alumina particles were measured at the required rotation speeds from −1.0 V to +0.7 V vs Hg/HgO at 1 mV/s with a pre-treatment at −1.5 V for 60 s prior to the initiation of potential sweep to remove any residual air-formed oxide film. The potential ramp was supplied to the controlling potentiostat by a linear sweep generator; whilst both potential and current measurements were taken at the data acquisition board and stored on the host computer.

2.4 Determinations of K_e, K_c and K_{ec}

The pure erosion component, K_e in the slurry was determined under protection condition so that only erosion can occur. The mass loss under effective cathodic protection (−0.9~−1.0 V) and at the potentials in-sufficiently negative to cause redeposition of dissolved iron[8,9] was taken to be the pure erosion rate, K_e.

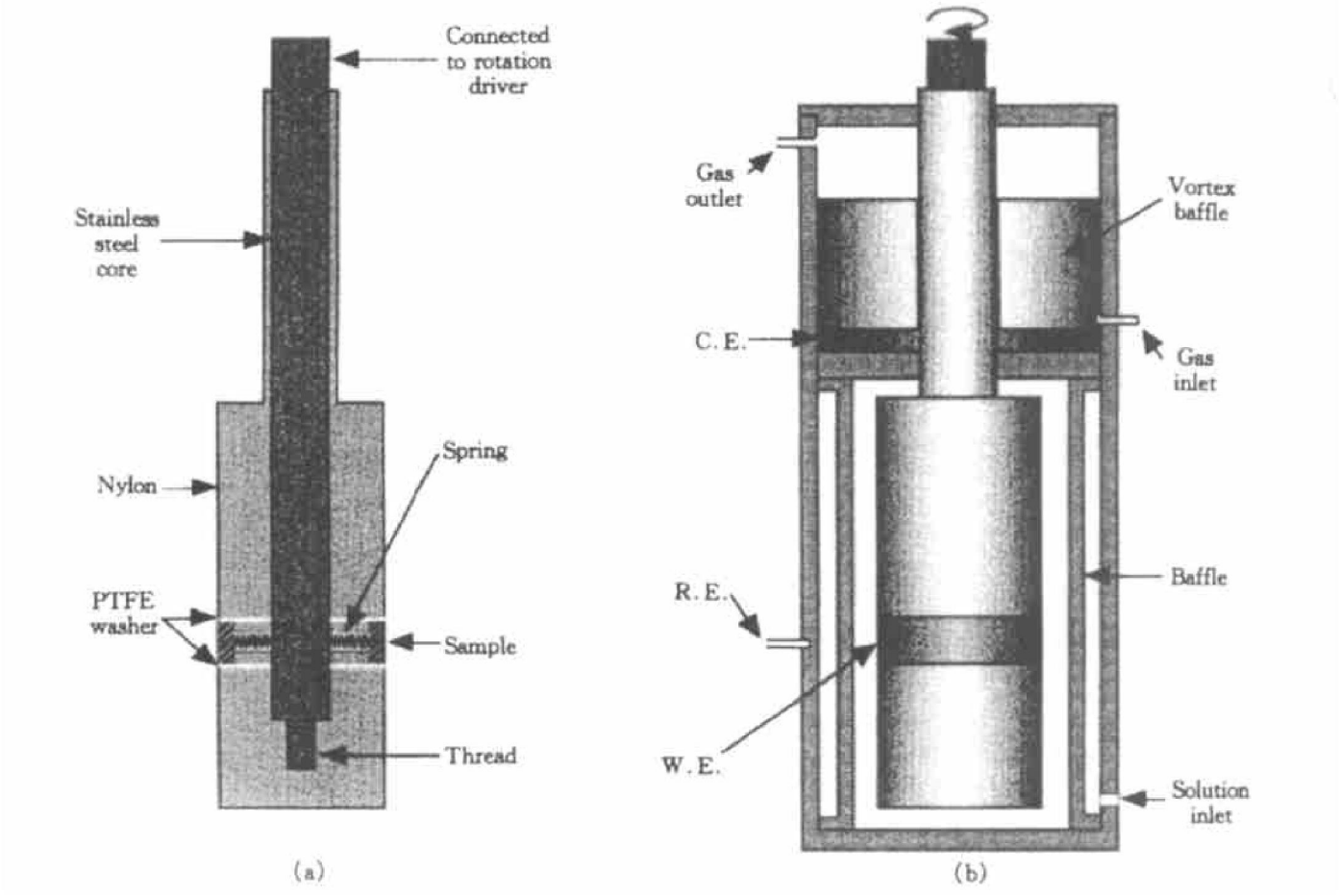

Fig. 1 Schematic diagram of rotating cylinder electrode system used for erosion-corrosion tests

Determination of the pure corrosion rate, K_c was carried out under the same conditions as for erosion-corrosion test and at the same potential to allow comparison. However, as the corrosion of chromium steel in sodium hydroxide is comparatively low, significant and measurable mass losses could only be made between + 0.2 V and + 0.6 V. The polarization potential and rotation were applied at the same time and data acquisition at a rate of 1 Hz started. The current was recorded for a period of 1 h until the test was stopped. The current data was integrated with respect to time to provide the quantity of change passed during the experiment, which in turn was used to provide a value for the corrosive mass loss using Faraday's second law [10].

The total erosion-corrosion rate (K_{ec}) at a given potential was measured as the total mass loss experienced by a sample during 1 h experiment in the presence of the required particulate concentration.

3 RESULTS AND DISCUSSION

3.1 Microstructure

In the annealed condition, the microstructure of the chromium steel consists of a matrix of fine ferrite grains with chromium carbides $(Fe, Cr)_7C_3$ dispersed in the grain boundaries. These precipitates have a minimum of 36% Cr and cause chromium content in regions adjacent to the phase boundaries to be lowered below the critical level 12% needed for corrosion resistance[11]. Therefore, the chromium steel is susceptible to intergranular and interphase corrosion. Fig. 2 shows that the surface morphology of the chromium steel was extensively pitted with evidence of general corrosion in 1 mol/L deaerated sodium hydroxide at a potential of + 0.4 V. The pits ranged in size from 2 μm to sub-micron with interior of the larger pits showing loose fibrous structures remaining after the preferential dissolution of ferrite phases and the original precipitate falling off.

3.2 Polarization curve

3.2.1 Effect of rotation speed

The measurement results of polarization curves for chromium steel in 1 mol/L sodium hydroxide solution with different rotation speeds are presented in Fig. 3. Compared with that of static state, the slight increase of passive current density in rotative state is the result of the joint action of acceleration of the transport process of the residual oxygen. An apparent positive shift of the free-corrosion potential occurred because the depolarization of oxygen became one of the main cathodic reactions in rotating state[12].

Without flow, the active peaks at − 0.8 V and − 0.6 V were decreased indicating less active dissolution while the ensuring passive region also resided at a lower current level, as a result of the chromium content allowing passivation to occur more easily and enhance the stability of the film formed. There was a large active peak developed at + 0.4 V due to the preferential dissolution of ferrite phase in chromium steel.

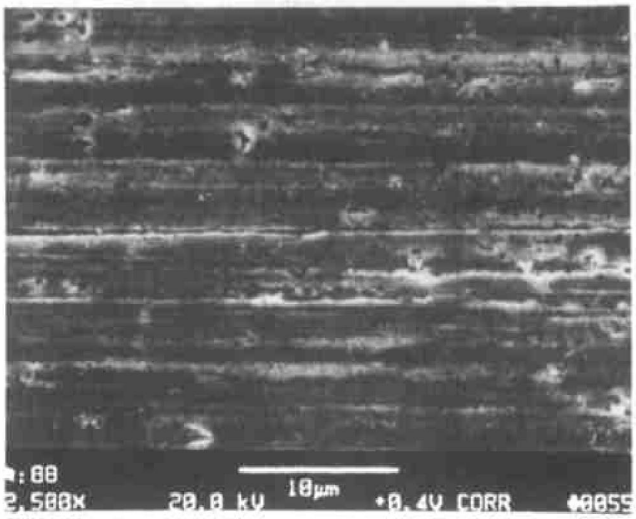

Fig. 2 Micrograph of chromium steel surface after erosion-corrosion test (rotation speed= 6 m/s)

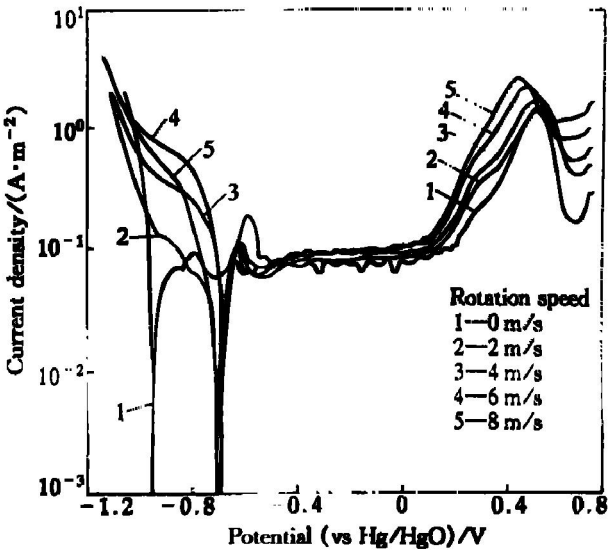

Fig. 3 Polarization behaviors for chromium steel in 1 mol/L NaOH solution with different rotation speeds

With cylinder rotation, the size of the active peak (at − 0.6 V) reduced with increasing rotation speed, possibly related to the transport of Fe ions, while the level of passivation current density(J_{pass}) increased sequentially with rotation speed as a result of the flow affecting the stability of the passive film. A stepwise increase with rotation speed was also noted over the potential range of the preferential dissolution (at + 0.4~ + 0.5 V) with the peak moving to slight more negative potentials at higher speeds.

3.2.2 Effect of particle size

Potentiodynamic scans were run to determine the effect of particle size on the polarization data. Fig. 4 shows the current density vs the polarization potential for chromium steel under test conditions of 6 m/s flow speed and 1 mol/L NaOH with 273 g/L alumina particles with different particle sizes.

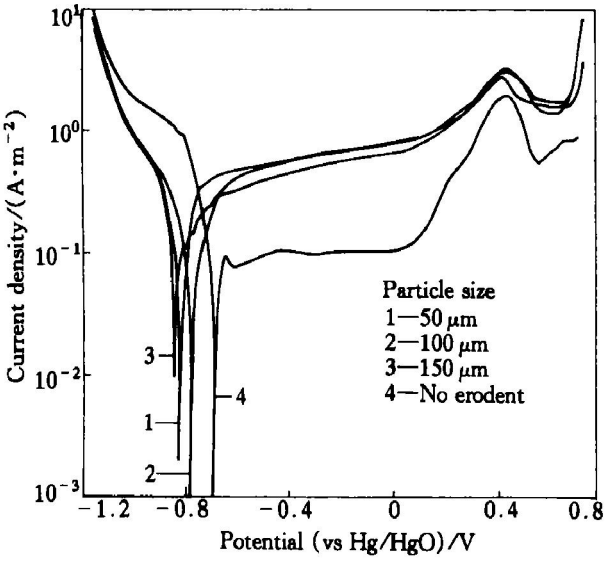

Fig. 4 Effect of particle size on polarization behavior of chromium steel

The addition of alumina particles increased the current density throughout the anodic potential region. And the presence of the small active peak was removed when no erodent particles were present, shifting the corrosion potential negatively by 0.10~0.15 V. The increase at the end of the passive region near 0 V was almost one order of magnitude regardless of the particle size added. It can be seen from Fig. 4 that the variation of particle size does not greatly affect the polarization behavior. The similarity despite differing particle sizes suggested that the effect on the electrochemical response produced by particle impacts was relatively constant. Thus the greater number of expected impacts for smaller particle sizes seems to compensate for the greater expected damage resulting from larger particle impacts. In the passive region equality in the current response occurred between 50 and 100 μm particles with the response for 150 μm being slightly lower. However, where active preferential dissolution of chromium steel at + 0.4 V occurred the responses for 100 and 150 μm particles were comparable with that for 50 μm being lower. It should be noted that the additions of alumina particles, compared with the solution without particles, accelerated the preferential dissolution of the ferrite phase.

3.3 Synergistic effect of erosion-corrosion

The variation of erosion-corrosion mass loss with potential and erodent particle size for chromium steel in de-aerated 1 mol/L NaOH at a rotation speed of 6 m/s with 273 g/L of alumina is shown in Fig. 5.

The increasing of electrochemical potential of

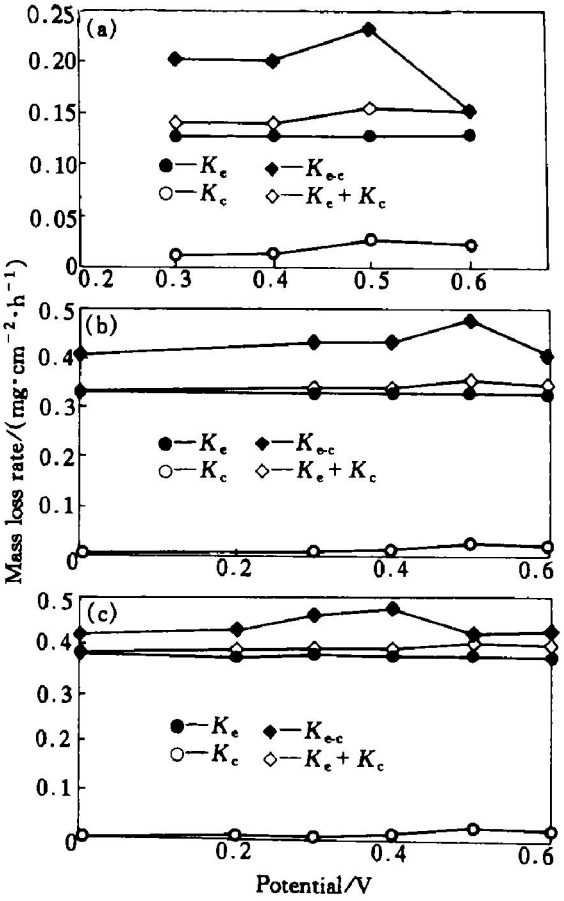

Fig. 5 Variation of erosion-corrosion mass loss with potential and erodent particle size for chromium steel
(a) —50 μm; (b) —100 μm; (c) —150 μm

samples had a pronounced effect on the pure corrosion rate, K_c and the erosion-corrosion rate, $K_{e\cdot c}$. Especially, as the potential of the test was moved anodically, the mass loss due to erosion-corrosion significant increased at the potential between + 0.4 V and + 0.5 V, where preferential dissolution was expected with reference to their respective polarization curves. In addition, a distinct variation in erosion-corrosion response was found with the three particle sizes tested. $K_{e\cdot c}$ was similar for both 100 and 150 μm erodent particles while for 50 μm particles it was approximately a third of that for the other size. This indicated that particle size enhanced the corrosion rate along with increased mass transfer. Moreover, erosion-corrosion rate ($K_{e\cdot c}$) was apparently higher than the sum (K_e+ K_c) of the pure erosion rate (K_e) and the pure corrosion rate (K_c).

As discussed above, the total synergism consists of two components: "corrosion increment" (ΔK_c) and "erosion increment" (ΔK_e). In present testing, the effect of erosion on corrosion includes the following two aspects[12]: the first is that erosion (flow) can enhance the transport process of both reactants

(such as the residual oxygen) reaching the metal surface which may improve the ability of passivation and repassivation of chromium steel and corrosion products leaving the metal surface which generally accelerate the corrosion process; the second is that erosion can apply a mechanical force on the metal surface which weakens and breaks the passive film on metal surface and results in an increase of internal energy which changes the surface activity of the metal and the formation of "strain difference cell"[13].

The main effect of corrosion on erosion is attributed to the preferential dissolution occurred in chromium steel. The preferential dissolution rate of ferrite phase at potential + 0.4~ + 0.5 V is large (as shown in Fig. 2) because of the depletion of main corrosion resistant element Cr in matrix which was caused by the deposition of $(Fe, Cr)_7C_3$. There is a potential difference between the ferrite phase and of $(Fe, Cr)_7C_3$. Their anodic curves show that in the vicinity of the corrosion potential for chromium steel, the $(Fe, Cr)_7C_3$ phase is more noble than the ferrite phase. Hence, this results in an accelerated corrosion rate for the ferrite phase and a protection of the $(Fe, Cr)_7C_3$ phase. The result of preferential dissolution enhances the erosion by the increase of surface roughness and also by the corrosion removal of the work hardened layer formed by erosion impacts. The synergism effect of erosion-corrosion decreases the bonding strength between the ferrite matrix and chromium carbide. The latter is gradually exposed and fall off under the frequent impact of abrasion[14]. This is one of the reason why pitting holes form and total mass loss increases at the potential between 0.4 V and 0.5 V. Meanwhile, it can be seen from Fig. 5 that the addition of particle enhances the synergism effect.

4 CONCLUSIONS

1) In the polarization curves, the position of the active peaks obtained by potentiodynamic measurements shows that preferential dissolution for the chromium steel containing 12% Cr occurs in 1 mol/L NaOH solution with and without particles. The ferrite phase is preferentially dissolved at the potential between + 0.4 V and + 0.5 V.

2) As the rotation speed increased, the potential peak of the preferential dissolution (at + 0.4~ + 0.5 V) moves to light more negative potential. It shows that the rotation speed is beneficial to preferential dissolution for chromium steel.

3) The additions of alumina particles, compared with the solution in the absence of particles, accelerate the preferential dissolution of the chromium steel. The variation of particle size does not greatly affect the polarization behavior. The responses for 100 μm and 150 μm particles occurred at + 0.4 V are comparable with that for 50 μm being lower.

[REFERENCES]

[1] Stack M M, Zhou S, Newman R C. Identification of transition in erosion-corrosion regimes in aqueous environments [J]. Wear, 1995, 186-187: 523-532.

[2] Zhou S, Stack M M, Newman R C. Electrochemical studies of anodic dissolution of mild steel in a carbonate-bicarbonate buffer under erosion-corrosion conditions [J]. Corrosion Science, 1996, 38(7): 1071-1084.

[3] Li Y, Burstein G T, Hutchings I M. The influence of corrosion on the erosion of aluminium by aqueous silica slurries [J]. Wear, 1995, 186-187: 515-522.

[4] Pitt C H, Chang Y M. Jet slurry corrosive wear of high-chromium cast iron and high carbon steel grinding ball alloys [J]. Corrosion, 1995, 42(6): 312-317.

[5] Matsumura M, Oka Y. Slurry erosion-corrosion of commercially pure Iron in fountain-jet testing facility [A]. 7th International Conference on Erosion by Liquid and Solid Impact[C]. Cambridge, UK, 1987, 40/1-40/8.

[6] Matsumura M. Erosion-corrosion of metallic materials in slurries [J]. Corrosion Reviews, 1994, 12(3-4): 321-340.

[7] Yue Z, Zhou P. Some factors influencing erosion-corrosion performance of materials [A]. Wear of Materials, ASME[C]. New York, USA, 1987, 763-768.

[8] Zhou S, Stack M M, Newman R C. Characterization of synergistic effects between erosion and corrosion in an aqueous environment using electrochemical technique[J]. Corrosion, 1996, 52(12): 934-946.

[9] Armstrong R D, Baurhoo I. The dissolution of iron in concentrated alkali [J]. Journal of Electroanalytical and Interfacial Electrochemistry, 1972, 40: 325-338.

[10] James J S. Investigations of aqueous erosion-corrosion using rotating cylinder electrodes[D]. UMIST, 1997.

[11] Smith W F. Structure and properties of engineering alloys [M]. Materials Science and Engineering Series, UK, 1991.

[12] Zheng Y G, Yao Z M, Wei X Y, et al. The synergistic effect between erosion and corrosion in acidic slurry medium [J]. Wear, 1995, 186-187: 555-561.

[13] Heidemeyer J. Influence of the plastic deformation of metals during mixed friction on their chemical reaction rate [J]. Wear, 1981, 66: 379-387.

[14] Wang R, Wang W C, Wang S Z, et al. A study of sand slurry erosion of W-alloy white cast irons [J]. Wear, 1993, 162: 259-254.

(Edited by YANG Bing)